FLOW DISPLACEMENT THROUGH NON-RECTILINEAR OIL WELLS

Jaques Savino, jaques.savino@petrobras.com.br
Mônica F. Naccache, naccache@puc-rio.br
Paulo R. de Souza Mendes, pmendes@puc-rio.br
Department of Mechanical Engineering
Pontifícia Universidade Católica do Rio de Janeiro
Rio de Janeiro, RJ 22453-900, Brasil

Abstract. *Flow through non-rectilinear annular spaces is found in fluid displacement processes during drilling, completion and gravel packing operations in horizontal oil wells. Some fluids employed in these processes, such as drilling muds and cement pastes, present a non Newtonian (viscoplastic) behavior, while the spacer fluids, used to avoid contamination, are Newtonian. The analysis of the flow displacement and of the interface configuration between these fluids helps to determine contamination and the displacement efficiency, and is an important tool for the process optimization. In this work we performed a numerical study to analyze the displacement of one fluid by another through a non-rectilinear annular channel, using Fluent Software (Ansys Inc.). The conservation equations of mass and momentum are solved via the finite volume technique, and the volume of fluid method. The effects of rheological parameters are investigated, for different flow rates and for two different situations, a viscoplastic liquid pushing a Newtonian one, and vice versa. When the viscoplastic liquid pushes the Newtonian one, the displacement efficiency decreases as we increase the velocity and the viscosity of the displaced fluid. Moreover, a fingering phenomenon is observed for higher velocities. On the opposite situation, when the Newtonian fluid pushes the viscoplastic one, the displacement efficiency increases with the velocity and viscosity of the displacer fluid, and the fingering is observed at lower flow rates.*

Keywords*: well cementing; fluid displacement; annuli; rheology; multiphase flow*

1. INTRODUCTION

Well constructions in offshore environments are related to high cost and risk. Exploratory trends advance to deep and ultra deep waters while the search for new sources leads to heavy oils reserves. In this scenario, long horizontal wells constitute economical drives for such field development. The development of horizontal drilling techniques began in the 70's, in the USA. Nowadays, horizontal well drilling is used in large scale in oil & gas reservoirs, to improve the contact area. Horizontal wells cost about three times more than the vertical ones, however the production can be increased up to twenty times. The main focus of this work is to optimize the relevant fluid displacement processes, which take place during drilling and completion phases of horizontal wells.

Cementing and cannonading long horizontal distances are critical and high cost operations. The usual technique of horizontal open wells completion in Brazil includes the pumping of gravel packs, as an additional barrier for sand containment. The technique of OHGP (Open Hole Gravel Packing) consists of placing a tube, with screens of special metallurgy, in the producing region of the wells. Therefore, a solid-liquid mixture is displaced, filling the annulus between the pipe and the wellbore.

The study of fluid displacement during drilling and completion is critical to obtain a good cementation process. Fluids with different physical properties (rheology and density) are used to improve the displacement efficiency, minimizing contamination and promoting hydrostatic column pressure to guarantee the operational window limits. Drilling mud, cement slurry and gravel pack present a viscoplastic behavior. Spacer fluids are also non Newtonian, with a shear thinning viscosity and washer fluids, usually a mixture of water and detergents, present a Newtonian behavior.

Previous studies about cementing wells focus the displacement of fluids in annuli. Clark & Carter (1973) and Haut & Crook (1978) observed that the effect of densities difference (buoyancy force) between mud and cement on the displacement efficiency is mild, but it is important for the generation of interface instabilities. The authors also showed that the displacement efficiency is larger in turbulent flows. Lockyear *et al.* (1990) described experiments in a large-scale flow loop. The velocity of the interface between fluids was analyzed, for different densities and rheological properties. The authors observed that severe channeling result, if the interface velocity on the wide side is substantially larger than that on the narrow side. The channeling can be minimized by the buoyancy mechanism and controlling stand-off of the casing. Guillot *et al.* (1990) performed a theoretical analysis using the lubrication theory in turbulent flows, to verify if the cement channeling through the drilling mud is reduced when spacer fluids are employed. The turbulent flow technique is limited by field operational conditions. Jakobsen *et al.* (1991) analyzed experimentally the effects of viscosity ratio, and buoyancy force of drilling fluid displacements in eccentric annulus. When the displacing fluid was 5% heavier than the displaced fluid, the static fluid moved from the narrow section up to the wide section of the annulus. This buoyancy-induced process strongly improved the displacement efficiency. Tehrani *et al.* (1992) performed a theoretical and experimental study of laminar flow of drilling fluids through eccentric annular spaces. They observed that the displacement efficiency decreases, as the eccentricity and the density difference increases.

The horizontal cementing process was analyzed in several studies in the literature. McPherson (2000) recommends at least a stand-off of 67%, to get good cementing hardenings. This stand-off allows a good mud removal and the correct placement of the cement. For horizontal wells some centralizers should be installed to get the specified stand-off. Kroken *et al.* (1996) developed a technique, called tide flow, for fluid displacements in eccentric horizontal annulus. In this technique, the potential energy of the slurry should, in every event, be greater than the kinetic energy. This technique is different of the traditional laminar displacement technique, which limits the fluid velocity on the wide side and considers density and friction pressure hierarchy. Bittleston *et al.* (2002) and Frigaard & Pelipenko (2003) present some theoretical results of cement displacement through eccentric annuli, considering two-dimensional laminar flows. They used the VOF (Volume of Fluid) model, with a Hele-Shaw approach, to show that the displacement front may reach permanent regime for some combinations of physical properties. Moyers-González *et al.* (2007) also used a Hele-Shaw model to simulate numerically the displacement of viscoplastic fluids in cementing operations. The authors investigated if the flow pulsation (in gradual waves) can reduce the mud channeling. After the beginning of the pulsation, the narrow mud channel slowly starts to flow off until it moves entirely. This process continues until the pulsation stops, when the mud comes back to be static. Dutra *et al.* (1995) presented a numerical simulation (VOF method) of fluid displacement in eccentric wellbores. The effect of the density difference and the rheology between fluids were analyzed, for a Newtonian fluid dislocating a non-Newtonian fluid (Herschel-Bulkley model), and vice versa. For the first case, the process is more efficient at higher flow rates. The eccentricity decreases the displacement efficiency, especially in horizontal geometries.

In this work, a two-phase tri-dimensional flow simulation is used to analyze the displacement process in horizontal wells. This is a complex problem, especially when one of the fluids presents non-Newtonian behavior, which is the most common situation. The displacement efficiency and the interface development were obtained numerically, using Fluent software (Ansys Inc.), for several combinations of the governing parameters.

2. MATHEMATICAL FORMULATION

The geometry analyzed is shown in Figure 1. The entrance is through a horizontal and axi-symmetric annulus, which connects to a zigzag tube. The geometry was based on the dimensions of an actual drilling well, in reduced scale. Before the beginning of the process simulation (t<0), the annular space is filled with fluid 1 (drilling or spacer fluid). At t=0, fluid 2 is injected at a constant flow rate, during a certain time interval.

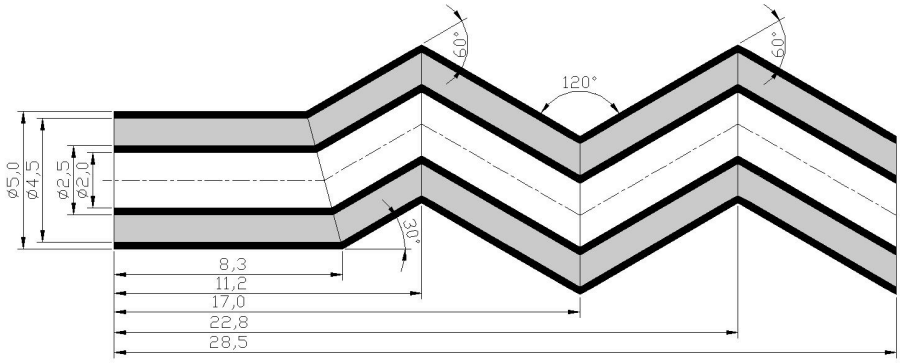

Figure 1. Zigzag geometry (section of flow, in grey)

The following hypotheses are considered: incompressible fluids, isothermal flow, negligible inertia and surface tension.

The volume of fluid method (VOF) (Fluent Users Guide, 2008 and Hirt & Nichols, 1981) is used to take into account the two-phase flow. The VOF formulation relies on the fact that two or more fluids (or phases) are not interpenetrating. As the phase volume cannot be share with other phases, the concept of the volumetric fraction (α_j) is introduced. These volume fractions are continuous functions in space and time, and the volume fractions of all phases sum to unity. Therefore, if:

- $\alpha_i = 0$, the volume does not contain the phase j;
- $\alpha_i = 1$, the volume contains only the phase j;
- $0 < \alpha_i < 1$, the volume contains the interface.

In this study, only two phases are present. The properties appearing in the transport equations, namely ϕ, are given by:

$$\phi = \alpha_2 \phi_2 + (1 - \alpha_2)\phi_1 \tag{1}$$

The interface between phases is obtained by the solution of the continuity equation for α_1:

$$\frac{\partial \alpha_1}{\partial t} + u_j \frac{\partial \alpha_1}{\partial x_j} = 0 \tag{2}$$

The volume fraction of the second phase is obtained with the following constraint equation:

$$\alpha_1 + \alpha_2 = 1 \tag{3}$$

The non-Newtonian (viscoplastic) behavior of the fluids is modeled by the Generalized Newtonian Fluid constitutive equation. Then, the stress tensor is given by: $\boldsymbol{\tau} = \eta(\dot{\gamma})\mathbf{D}$, where $\mathbf{D} = \left(\nabla \mathbf{v} + (\nabla \mathbf{v})^T\right)$ is the rate-of-strain tensor, **v** is the velocity vector and $\dot{\gamma} = \sqrt{1/2 \mathrm{tr}\mathbf{D}^2}$ is the magnitude of the rate-of-strain tensor. Therefore, the momentum equation is given by:

$$\frac{\partial(\rho u_i)}{\partial t} + \frac{\partial(\rho u_i u_k)}{\partial x_i} = -\frac{\partial p}{\partial x_k} + \frac{\partial}{\partial x_i}\left[\eta\left(\frac{\partial u_i}{\partial x_k} + \frac{\partial u_i}{\partial x_i}\right)\right] + \rho g_k \tag{4}$$

In the above equation, x_j are the coordinates, u_j are the velocity components, *t* is the time, p is the pressure, ρ is the density and η is the viscosity function. ρ and η are shared between phases in momentum equation using the volume fraction. The viscosity function is given by the SMD equation, proposed by Souza Mendes & Dutra (2004):

$$\eta = \left\{1 - \exp\left(\frac{-\eta_0 \dot{\gamma}}{\tau_0}\right)\right\}\left[\frac{\tau_0}{\dot{\gamma}} + k\dot{\gamma}^{n-1}\right] \tag{5}$$

The SMD equation can be better understand with the aid of Figure 2. The viscosity is continuous, with a high zero-shear rate plateau for low deformation rates, equal to η_0, followed by a sharp drop at the yield stress τ_0(or at $\dot{\gamma} = \dot{\gamma}_0$). After $\dot{\gamma} = \dot{\gamma}_1$ the viscosity presents a power-law behavior, with a consistency index equal to *k* and a power-law index equal to *n*.

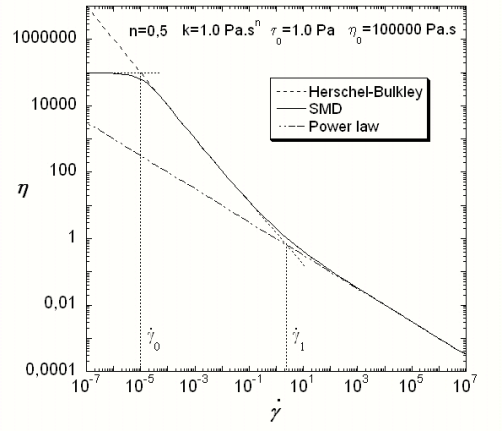

Figure 2. Comparative graph between rheological models

The transition values of the deformation rate are obtained from the rheological parameters, and are given by:

$$\dot{\gamma}_0 \equiv \frac{\tau_0}{\eta_0} \qquad \dot{\gamma}_1 \equiv \left(\frac{\tau_0}{k}\right)^{\frac{1}{n}} \tag{6}$$

(7)

The governing parameters of the problem are defined with the aid of the dimensionless equations, obtained using the following dimensionless variables:

$$x_i^* \equiv \frac{x_i}{D_o - D_i} \qquad v_i^* \equiv \frac{v_i}{\dot{\gamma}_1 (D_o - D_i)} \qquad \hat{t} \equiv \dot{\gamma}_1 t$$

$$p^* \equiv \frac{p}{\rho \dot{\gamma}_1^2 (D_o - D_i)^2} \qquad \tau^* \equiv \frac{\tau}{\tau_0} \qquad \eta^* \equiv \frac{\eta}{\tau_0 / \dot{\gamma}_1} \qquad \dot{\gamma}^* \equiv \frac{\dot{\gamma}}{\dot{\gamma}_1}$$

D_o and D_i are the outer and inner diameters of the annulus, respectively. The dimensionless variables described above are chosen accordingly to Souza Mendes (2007). The resulting dimensionless rheological groups/variables are given by:

- The Reynolds number: $\mathrm{Re} \equiv \frac{\rho \dot{\gamma}_1^2 (D_o - D_i)^2}{\tau_0}$
- The Galilei number: $Ga \equiv \frac{g}{\dot{\gamma}_1^2 (D_o - D_i)}$
- The Jump number: $J \equiv \frac{\dot{\gamma}_1 - \dot{\gamma}_0}{\dot{\gamma}_0} = \frac{\eta_0 \tau_0^{(1-n)/n}}{k^{1/n}} - 1$
- The power-law index: n

Boundary conditions

The geometry and mesh of the three-dimensional model were developed in software GAMBIT (Figure 3). The boundary conditions were:

- **Inlet** – prescribe velocity with uniform profile;
- **Outflow** – fully-developed flows (zero diffusion flux for all flow variables);
- **Wall** – no-slip and impermeability;
- **Symmetry** – Zero normal velocity and zero normal gradients of all variables.

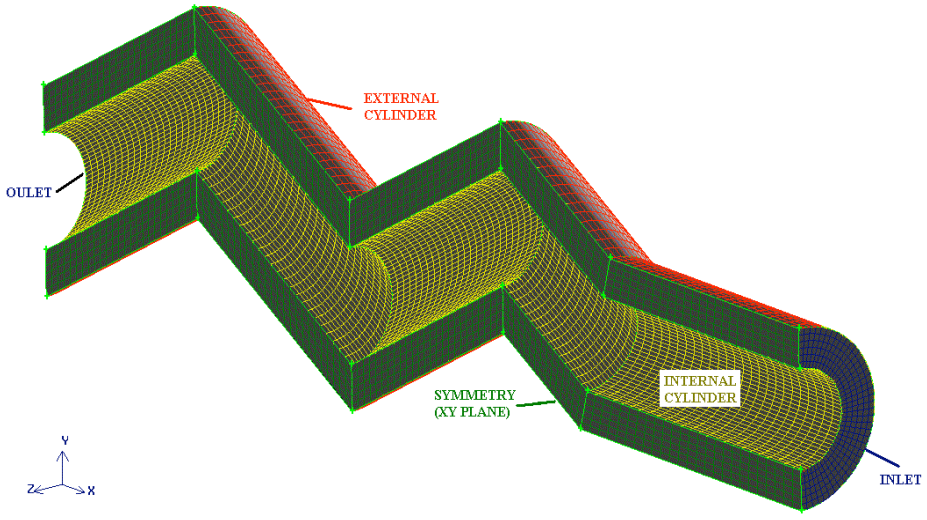

Figure 3 – 3D Mesh and boundary conditions.

3. NUMERICAL FORMULATION

The governing equations presented above were discretized via the finite volume method described by Patankar (1980), using the SIMPLE algorithm (Patankar, 1980) to couple velocity and pressure. The numerical solution was obtained using FLUENT software (Ansys Inc.), using and iterative time step evolution procedure and the following discretization/linearization schemes:

- Pressure: PRESTO!
- Momentum: First Order Upwind
- Volume Fraction: Geo-Reconstruct
- Time: First Order Implicit

To validate the numerical modeling, a flow visualization was performed, together with the evaluation of the displacement efficiency, measured by the relation between the dimensionless volume of the displaced liquid remaining inside the annular ($V^* = V/V_{annular}$), and a dimensionless time $t^* \equiv u_E \cdot t/L$. In this definition, u_E is the inlet prescribed velocity, t is the total pumping time and L is the pipe length. Therefore, $V^*=100\%$ at $t^*=1$ if the displacement is perfect, i.e., if the displacer fluid flows like a plug. The following tests had been carried out:

- **Mesh refinement test**: three different 3D meshes sizes were tested, using two Newtonian fluids: 5280, 27600 and 69120 elements. The mesh with 27600 elements was chosen, since the difference in the displacement efficiency between this mesh and the refined mesh was below 0.03% for the two cases analyzed. Moreover, flow visualization results showed the same behavior.
- **Time step test**: three different time steps were tested, using the mesh chosen above and two Newtonian fluids: 0.0025s, 0.0050s e 0.0100s. The time step of 0.0050s was chosen, since the difference in the displacement efficiency between this case and the one with the time step equal to 0.0025s was below 0.15% for the two cases analyzed.
- **Viscosity model**: the viscosity equation was defined in Fluent using an UDF - *User-Defined Function* (Fluent Users Guide, 2008). Therefore, some 2D tests were accomplished in order to verify the implementation. The velocity profile, the deformation rate and the viscosity were compared with a semi-analytical result, for three different flow rates, showing a very good agreement.

4. RESULTS

Simulations of two fluids displacements had been carried out. In the first situation, the displacer fluid (non-Newtonian) simulates the cement slurry (or gravel pack) while the displaced fluid (Newtonian) simulates the spacer or washer fluid. In the second situation, the displacer fluid (Newtonian) simulates the spacer or washer fluid, while the displaced fluid (non-Newtonian) simulates the drilling mud.

The inertia was considered negligible (Re << 1) and the Galilei number was also neglected. The displacements had been analyzed varying the (dimensionless) rheological properties and the dimensionless inlet velocity, to determine the influence of these parameters in the displacement efficiency, as follows:

Table 1. Displacement parameters

	μ
Newt-I	0.1
Newt-II	1.0
Newt-III	10.0

Rheology - Newtonian fluid

	n	J
NNewt-A	1.0	100000
NNewt-B	0.5	100000

Rheology - non-Newtonian fluid

	u^*
Velocity-1	0.1
Velocity-2	1.0
Velocity-3	10.0

Velocity

From these variables, 36 cases were determined to be simulated (Tables 2 and 3). The results are shown and compared in terms of a quantitative evaluation of the displacement efficiency, defined in the section before. A qualitative evaluation of the displacement is also carried out by images of the interface profile between two phases, on a wireframe 3D model, for three different dimensionless times.

4.1. Non-Newtonian fluid displacing Newtonian fluid

Table 2 shows the 18 simulated cases for non-Newtonian displacing Newtonian fluids, as well as the efficiency at $t^* = 1.0$. The displacer fluid (non-Newtonian) simulates the cement slurry (or gravel pack) while the displaced fluid (Newtonian) simulates the washing fluid.

Table 2. Simulating cases: non-Newtonian displacing Newtonian fluids

CASE		NON-NEWTONIAN → NEWTONIAN	VELOCITY	EFFICIENCY
CASE I	1A	NN (n=1.0) → N (μ=0.1)	0.1	98%
	1B	NN (n=0.5) → N (μ=0.1)		98%
	2A	NN (n=1.0) → N (μ=0.1)	1.0	89%
	2B	NN (n=0.5) → N (μ=0.1)		89%
	3A	NN (n=1.0) → N (μ=0.1)	10.0	87%
	3B	NN (n=0.5) → N (μ=0.1)		85%
CASE II	1A	NN (n=1.0) → N (μ=1.0)	0.1	87%
	1B	NN (n=0.5) → N (μ=1.0)		87%
	2A	NN (n=1.0) → N (μ=1.0)	1.0	84%
	2B	NN (n=0.5) → N (μ=1.0)		83%
	3A	NN (n=1.0) → N (μ=1.0)	10.0	83%
	3B	NN (n=0.5) → N (μ=1.0)		73%
CASE III	1A	NN (n=1.0) → N (μ=10)	0.1	79%
	1B	NN (n=0.5) → N (μ=10)		80%
	2A	NN (n=1.0) → N (μ=10)	1.0	71%
	2B	NN (n=0.5) → N (μ=10)		64%
	3A	NN (n=1.0) → N (μ=10)	10.0	70%
	3B	NN (n=0.5) → N (μ=10)		53%

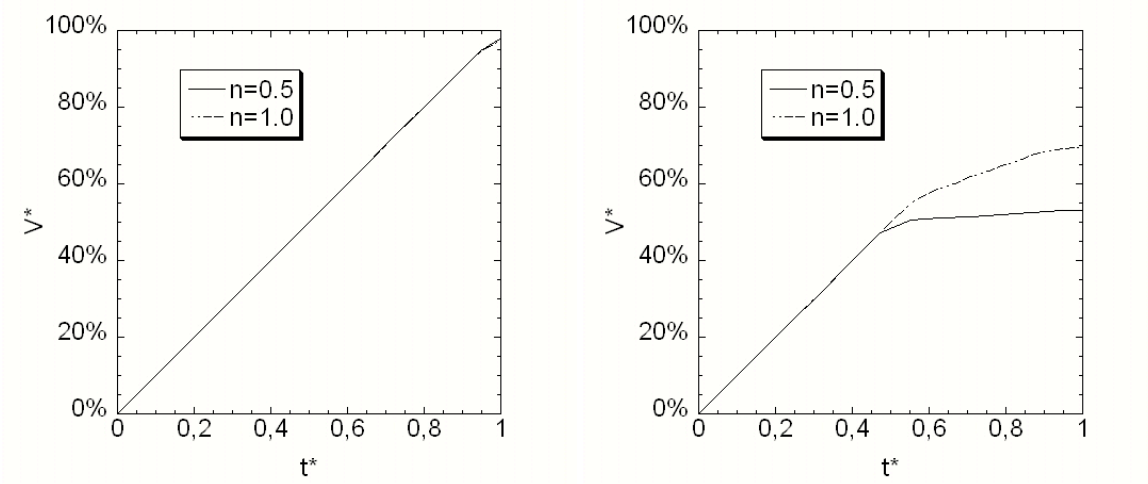

Figure 4. Efficiency displacement for non-Newtonian displacing Newtonian fluid: (a) Cases I (n=0.5 and 1.0, μ=0.1, u^*=0.1); (b) Cases III (n=0.5 and 1.0, μ=10, u^*=10).

Figure 4 shows the displacement efficiency for Cases I (n=0.5 and 1.0, μ=0.1, and dimensionless inlet velocity equal to 0.1) and III (n=0.5 and 1.0, μ=10, and inlet velocity equal to 10). It can be observed that the displacement efficiency is better for Cases I, since the inlet velocities are lower (and so the viscosity of the displacer fluid, which is non Newtonian, is higher). Moreover, in this case the viscosity of the displaced fluid is low (μ=0.1). It is well know from the literature that when the viscosity of the displacer fluid is larger than the viscosity of the displaced fluid, a plug flow of the displacer fluid is expected, leading to better displacement efficiencies. However, if the opposite occurs the channeling or fingering phenomenon is expected to occur, resulting in poor displacement processes. Therefore, in Cases I, the two variables (inlet velocity and Newtonian viscosity) are leading to a more favorable viscosity ratio between the displacer and displaced fluids, resulting in a more efficient displacement process. Increasing the Newtonian viscosity

and the inlet velocity, the displacement efficiency decreases, since worse viscosity ratios are obtained. This behavior repeats for all cases analyzed, as it can be noted with the aid of Table 2.

Figures 5 and 6 show the interface profile between two phases for three different dimensionless times, for Cases I and III, respectively. It can be observed that the interface is almost flat for the lower Newtonian viscosity and inlet velocity, similar to a plug flow, as expected. However, flow channeling is observed for the higher Newtonian viscosity and inlet velocity (Cases III).

CASE I	$t^* = 0.3$	$t^* = 0.6$	$t^* = 1.0$
1A	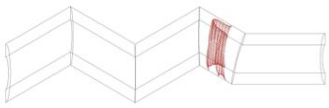	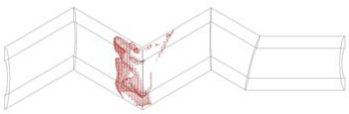	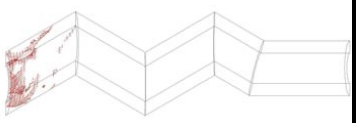
1B	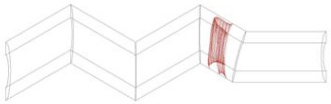	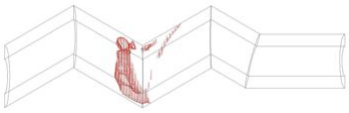	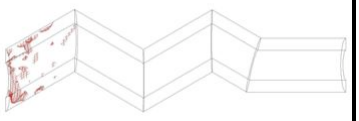

Figure 5. Interface for non-Newtonian displacing Newtonian fluid for Cases I (n=0.5 and 1.0, μ=0.1, u^*=0.1).

CASE III	$t^* = 0.3$	$t^* = 0.6$	$t^* = 1.0$
3A	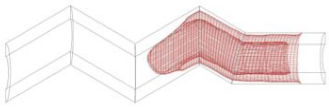	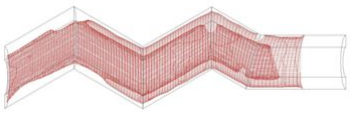	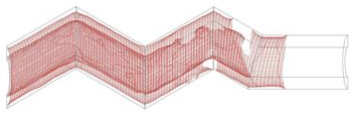
3B	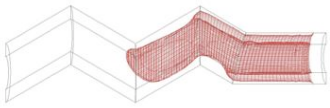	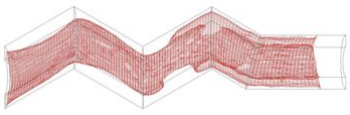	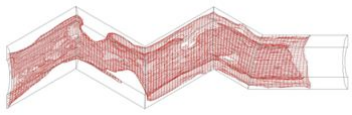

Figure 6. Interface for non-Newtonian displacing Newtonian fluid for Cases III (n=0.5 and 1.0, μ=10, u^*=10).

4.2 Newtonian fluid displacing non-Newtonian fluid

Table 3 shows the 18 simulated cases for Newtonian displacing non-Newtonian fluids, as well as the efficiency after $t^* = 1.0$. The displacing fluid (Newtonian) simulates the washer while the dislocated fluid (non-Newtonian) simulates the drilling mud. Based on table 3, some representative cases will be analyzed in detail. Figure 7 shows the displacement efficiency for these cases, and Figures 8 and 9 show the interface configuration for the same cases.

It can be observed that the efficiency displacement is lower for lower Newtonian viscosities. As we increase the inlet velocity, the displacement becomes more efficient, since the non-Newtonian viscosities decreases, and so the viscosity ratio between the displaced and displacer fluids decreases. Figures 8 and 9 show the interface profile between the two phases for three different dimensionless times. The channeling process can be observed for the less efficiency cases (μ=0.1, u^*=0.1). However, the plug flow occurs for the cases with a more favorable viscosity ratio, or higher Newtonian viscosity and inlet velocity (μ=10, u^*=10).

Table 3. Simulating cases: Newtonian displacing non-Newtonian fluids

CASE		NEWTONIAN → NON-NEWTONIAN	VELOCITY	EFFICIENCY
CASE IV	1A	N (μ=0.1) → NN (n=1.0)	0.1	52%
	1B	N (μ=0.1) → NN (n=0.5)		50%
	2A	N (μ=0.1) → NN (n=1.0)	1.0	66%
	2B	N (μ=0.1) → NN (n=0.5)		61%
	3A	N (μ=0.1) → NN (n=1.0)	10.0	69%
	3B	N (μ=0.1) → NN (n=0.5)		80%
CASE V	1A	N (μ=1.0) → NN (n=1.0)	0.1	71%
	1B	N (μ=1.0) → NN (n=0.5)		67%
	2A	N (μ=1.0) → NN (n=1.0)	1.0	82%
	2B	N (μ=1.0) → NN (n=0.5)		85%
	3A	N (μ=1.0) → NN (n=1.0)	10.0	83%
	3B	N (μ=1.0) → NN (n=0.5)		88%
CASE VI	1A	N (μ=10) → NN (n=1.0)	0.1	88%
	1B	N (μ=10) → NN (n=0.5)		87%
	2A	N (μ=10) → NN (n=1.0)	1.0	88%
	2B	N (μ=10) → NN (n=0.5)		91%
	3A	N (μ=10) → NN (n=1.0)	10.0	88%
	3B	N (μ=10) → NN (n=0.5)		97%

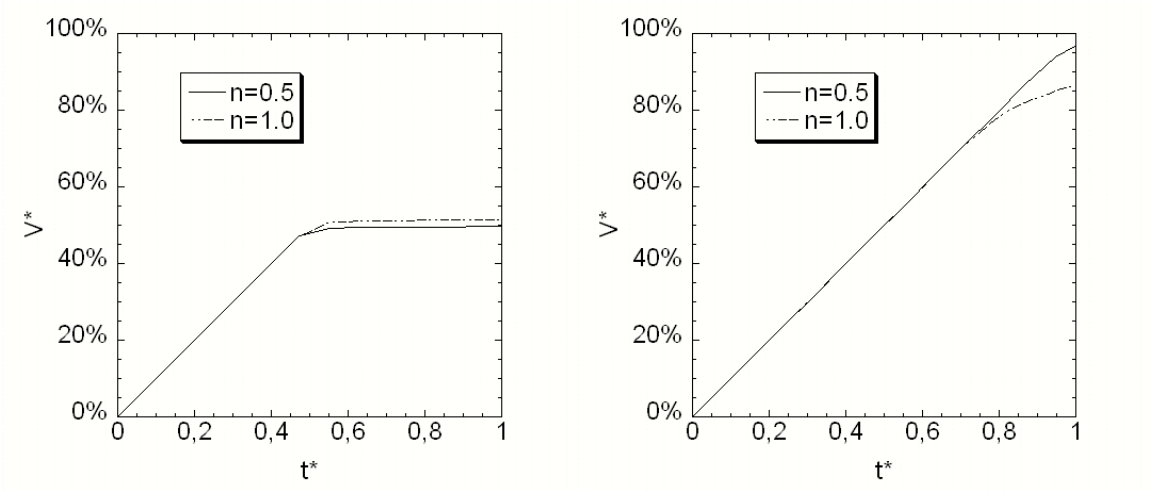

Figure 7. Efficiency displacement for Newtonian displacing non-Newtonian fluid: (a) Cases IV (n=0.5 and 1.0, μ=0.1, u^*=0.1); (b) Cases VI (n=0.5 and 1.0, μ=10, u^*=10).

CASE IV	$t^* = 0.3$	$t^* = 0.6$	$t^* = 1.0$
1A	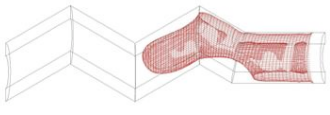	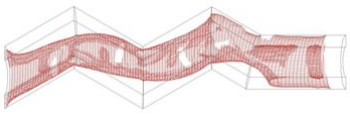	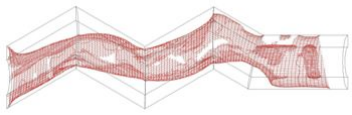
1B	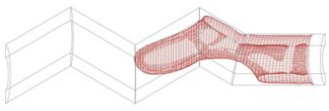	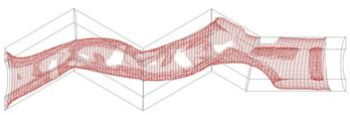	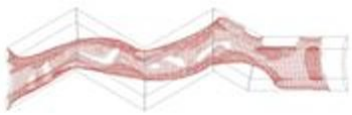

Figure 8 – Interface for Newtonian displacing non-Newtonian fluid for Cases IV (n=0.5 and 1.0, μ=0.1, u^*=0.1).

CASE VI	$t^* = 0.3$	$t^* = 0.6$	$t^* = 1.0$
3A	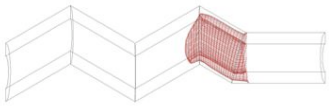	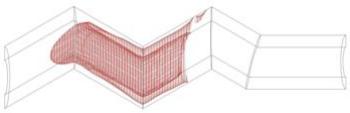	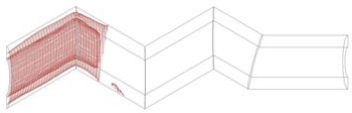
3B	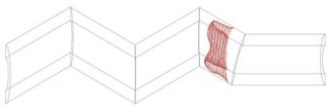	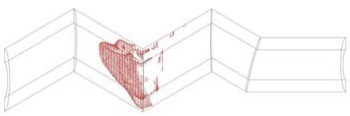	

Figure 9. Interface for Newtonian displacing non-Newtonian fluid for Cases VI (n=0.5 and 1.0, μ=10, u^*=10).

5. FINAL REMARKS

In this work, we studied numerically the flow displacement of two fluids through a non-rectilinear tube, as an attempt to describe and optimize fluid displacement processes during drilling, completion and gravel packing operations in horizontal oil wells. The governing equations were solved via the finite volume technique, using the volume of fluid method and the Fluent software (Ansys Inc.). The results were obtained for two different situations: a non-Newtonian fluid displacing a Newtonian one and vice-versa. The effect of some governing parameters on the displacement efficiency was determined and analyzed, with the aid of the visualization of the interface evolution through the tube.

The results showed that better displacements are obtained when the ratio between the viscosities of the displacer fluid to the displaced one is larger than unity, and increases as we increase it. When this ratio is lower than unity the channeling or fingering phenomenon occurs, leading to lower displacement efficiencies. It was also showed that the power law index has almost no effect on the displacement process.

This research is still in progress, and future topics to be investigated are: the effect of density differences between fluids, incorporating the buoyancy forces as a parameter; perform some experimental tests in reduced scale in order to validate the numerical solution.

6. REFERENCES

Bittleston, S. H.; Ferguson, J.; Frigaard, I. A., 2002, "Mud Removal and Cement Placement During Primary Cementing of an Oil Well Laminar non-Newtonian Displ. in an Ecc. Annular Hele-Shaw Cell". J. Eng. Math., 43, 229-253.

Clark, C. R.; Carter, L. C., 1973, "Mud Displacement with Cement Slurries". J. Petr. Tech., 25 (7), 775-783.

Dutra E. S. S.; Martins, A. L.; Miranda, C. R.; Aragão, A. F. L.; Mendes, P. R. S.; Naccache, M. F., 2005, "Dynamics of Fluid Substitution While Drilling and Completing Long Horizontal-Section Wells". SPE.

Guillot, D. J; Couturier, M.; Hendriks, H.; Callet, F., 1990, "Design Rules and Associated Spacer Properties for Optimal Mud Removal in Eccentric Annuli". SPE.

Haut, R. C.; Crook, R. J., 1978, "Primary Cementing: The Mud Displacement Process", SPE, 23-26.

Hirt, C. W.; Nichols, B. D., 1981, "Volume of Fluid (VOF) Method for the Dynamics of Free Boundary" J. Comp. Physics, 39, 204-225.

Jakobsen, J.; Sterri, N.; Saasen, A.; Aas, B., 1991, "Displacements in Eccentric Annuli During Primary Cementing in Deviated Wells". SPE.

Kroken, W.; Sjtiholm, J.; Olsen, A. S., 1996, "Tide Flow: A Low Rate Density Driven Cementing Technique for Highly Deviated Wells". SPE.

Lockyear, C. F., Ryan, D. F.; Gunningham, M. M., 1990, "Cement Channeling: How to Predict and Prevent". SPE Drilling Eng., 5 (3), 201-208.

Mcpherson, S. A., 2000, "Cementation of Horizontal Wellbore". SPE.

Moyers-González, M. A.; Frigaard, I. A.; Scherzer, O.; Tsai, T.-P., 2007, "Transient Effects in Oilfield Cementing Flows: Qualitative Behaviour. European" J. Appl. Math., 18, 477–512.

Souza Mendes, P. R.; Dutra, E. S. S., 2004, "Viscosity Function for Yield Stress Liquids". Appl. Rheology. 14 (6), 296–302.

Souza Mendes, P. R., 2007, "Dimensionless non-Newtonian Fluid Mechanics", J. Non-Newtonian Fluid Mech., 147, 109-116.

Tehrani, A.; Ferguson, J.; Bittleston, S. H., 1992, Laminar Displacement in Annuli: A Combined Experimental and Theoretical Study. SPE.

7. RESPONSIBILITY NOTICE

The authors are the only responsible for the printed material included in this paper.